

# Density Profiles in a Classical Coulomb Fluid Near a Dielectric Wall. I. Mean-Field Scheme

Jean-Noël Aqua<sup>1</sup> and Françoise Cornu<sup>1</sup>

*Received November 14, 2000; revised May 11, 2001*

---

The equilibrium density profiles in a classical multicomponent plasma near a hard wall made with a dielectric material characterized by a relative dielectric constant  $\epsilon_w$  are studied from the first Born–Green–Yvon (BGY) equation combined with Poisson equation in a regime where Coulomb coupling is weak inside the fluid. In order to prevent the collapse between charges with opposite signs or between each charge and its dielectric image inside the wall when  $\epsilon_w > 1$ , hard-core repulsions are added to the Coulomb pair interaction. The charge-image interaction cannot be treated perturbatively and the density profiles vary very fast in the vicinity of the wall when  $\epsilon_w \neq 1$ . The formal solution of the associated inhomogeneous Debye–Hückel equations will be given in Paper II, together with a systematic fugacity expansion which allows to retrieve the results obtained from the truncated BGY hierarchy. In the present paper the exact density profiles are calculated analytically up to first order in the coupling parameter. The expressions show the interplay between three effects: the geometric repulsion from the impenetrable wall; the electrostatic effective attraction ( $\epsilon_w > 1$ ) or repulsion ( $\epsilon_w < 1$ ) due to its dielectric response; and the Coulomb interaction between each charge and the potential drop created by the electric layer which appears as soon as the system is not symmetric. We exhibit how the charge density profile evolves between a structure with two oppositely-charged layers and a three-layer organization when  $\epsilon_w$  varies. (The case of two ideally conducting walls will be displayed elsewhere).

---

**KEY WORDS:** Coulomb interactions; dielectric wall; BGY equation; inhomogeneous Debye–Hückel equation; electric layer.

---

<sup>1</sup>Laboratoire de Physique Théorique (Laboratoire associé au Centre National de la Recherche Scientifique - UMR 8627), Bâtiment 210, Université Paris-Sud, 91405 Orsay Cedex, France; e-mail: Francoise.Cornu@th.u-psud.fr

## 1. INTRODUCTION

The present paper provides new exact analytical perturbative results for the density profiles of a classical Coulomb plasma in the vicinity of a polarizable boundary. We consider a multicomponent plasma, namely a system made of at least two species of moving charges with opposite signs. The linear electrostatic response of the wall is described at a macroscopic level by a relative dielectric constant  $\epsilon_w$ . ( $\epsilon_w$  is the ratio of the dielectric constants in the wall and in the half-space occupied by the Coulomb fluid). The density profiles are obtained in a high-temperature (or low-density) limit which is realized for instance in an electrolyte solution.

As shown in Paper II—published just after the present paper—this limit is the first-order result in a systematic expansion in powers of the Coulomb coupling parameter. This limit can be retrieved from a mean-field approximation for the first Born–Green–Yvon (BGY) equation which leads to the resolution of inhomogeneous Debye–Hückel equations. For the sake of pedagogy, the present paper is devoted to the mean-field interpretation, which should be more familiar to readers interested in chemical physics, and to the discussion of the properties of the electric layer. The exact derivation is postponed to Paper II where we present two points: first, systematic resummations of Coulomb divergencies in the framework of the grand-canonical ensemble; second, the resolution of the inhomogeneous Debye–Hückel equations obeyed by the auxiliary effective potentials which arise from the latter resummations.

The Coulomb pair interaction  $v(\mathbf{r}; \mathbf{r}')$  between two unit charges located respectively at  $\mathbf{r}$  and  $\mathbf{r}'$  near the dielectric wall, namely the solution of Poisson equation

$$\Delta_{\mathbf{r}} v(\mathbf{r}; \mathbf{r}') = -4\pi\delta(\mathbf{r} - \mathbf{r}') \quad (1.1)$$

with the adequate electrostatic boundary conditions, reads

$$v_w(\mathbf{r}; \mathbf{r}') = \frac{1}{|\mathbf{r} - \mathbf{r}'|} - \Delta_{\text{el}} \frac{1}{|\mathbf{r} - \mathbf{r}'^*|} \quad (1.2)$$

where  $\Delta_{\text{el}} \equiv (\epsilon_w - 1)/(\epsilon_w + 1)$  and  $\mathbf{r}'^*$  is the image of  $\mathbf{r}'$  with respect to the plane interface.<sup>(7)</sup> When  $\epsilon_w$  varies from 0 to  $+\infty$ ,  $\Delta_{\text{el}}$  ranges from  $-1$  to  $1$ . In a dielectric material  $-1 < \Delta_{\text{el}} < 1$ . If the Coulomb fluid mimics an electrolyte in a solvent described as a rigid continuum medium,  $\epsilon_w$  is the relative dielectric constant of the wall with respect to the solvent dielectric constant  $\epsilon_s$  and the interaction potential  $v_w$  in (1.2) is to be multiplied by

$1/\epsilon_s$ . The potential (1.2) may be seen as the sum of two contributions. The vacuum or “bulk” potential

$$v_B(\mathbf{r}; \mathbf{r}') = \frac{1}{|\mathbf{r} - \mathbf{r}'|} \quad (1.3)$$

is the solution of (1.1) far away from any boundary or in the vicinity of a wall with no electrostatic response ( $\epsilon_w = 1$ ). The second term in (1.2) is the interaction with an “image” charge; the latter describes the interaction with the polarization charge generated in the material by plasma charges. The corresponding self-energy of a charge  $e_\alpha$  at point  $\mathbf{r}$ —namely the work needed to take one charge  $e_\alpha$  from the bulk to point  $\mathbf{r}$  in the vicinity of the wall—is equal to  $e_\alpha^2 V_{\text{self}}(\mathbf{r})$  with

$$V_{\text{self}}(\mathbf{r}) = \frac{1}{2} [v_w - v_B](\mathbf{r}, \mathbf{r}) \quad (1.4)$$

In (1.4) the factor  $1/2$  in the interaction between a charge and its image comes from the proportionality between the two charges. In the following, the interface is perpendicular to the  $x$ -axis and located at  $x=0$ , and, according to (1.2),

$$V_{\text{self}}(x) = -\Delta_{\text{el}} \frac{1}{4x} \quad (1.5)$$

When  $\Delta_{\text{el}} > 0$  a hard-core repulsion from the wall must be introduced in order to prevent the collapse of each charge with its image. For the sake of simplicity, the range  $b$  of the repulsion from the wall is chosen to be the same for all species in the present paper. Even in the bulk, a short-distance cut-off must be introduced in order to prevent the collapse of the system due to the attraction between charges with opposite signs. However this second cut-off proves not to arise in the densities at leading order in the Coulomb coupling parameter inside the fluid. (Indeed, in the first BGY hierarchy the variation of the density of every species depends on correlations only through an integral and the value of the latter integral at leading order in the Coulomb coupling parameter is determined only by the behavior of correlations at distances far larger than the short-distance cut-off.)

For a long time, the short-distance singularity of the charge-image interaction has prevented one from getting exact results in the case  $\epsilon_w \neq 1$  at any distance from the wall for either a generic multicomponent or a One-Component Plasma (OCP), namely a system made of only one moving

charge species in a rigid neutralizing background. The self-consistent method introduced by Guernsey<sup>(6)</sup> for a plain wall ( $\epsilon_w = 1$ ) was generalized for the first time to a case where  $\epsilon_w \neq 1$  by Alastuey.<sup>(1)</sup> This author dealt with the OCP near a wall with a repulsive electrostatic response ( $\epsilon_w < 1$ ) in the weak-coupling limit. In this case the density vanishes on the wall and drastically varies over the closest approach distance  $\beta e^2$ . The mean-field electrostatic potential  $\Phi(x)$  created by the charge density profile is solution of an inhomogeneous Debye–Hückel equation where the inverse Debye length depends on the distance from the wall and rapidly varies in its vicinity. Alastuey solved the equation for the mean-field value of  $\Phi(x)$  and produced the corresponding profile density but only for distances larger than the closest approach distance. (For these distances a linearization may be performed and the equation for  $\Phi(x)$  becomes a second-order linear differential equation with constant parameters). The case  $\epsilon_w > 1$ , where the attractive response of the wall makes the density diverge exponentially fast on the wall in the absence of any hard-core repulsion, was left unsolved at any distance.

In Section 2 we introduce a self-consistent scheme for the determination of density profiles in a multicomponent plasma from the first BGY equation combined with Poisson equation. By using the results of Paper II about the solutions of the corresponding inhomogeneous Debye–Hückel equations, we give their formal expressions *at any distance* from the wall at first order in the coupling parameter  $\epsilon_D$  inside the fluid,

$$\epsilon_D \equiv \frac{1}{2} \beta e^2 \kappa_D \quad (1.6)$$

In (1.6)  $\beta$  is the inverse temperature,  $\beta = 1/k_B T$  where  $k_B$  is Boltzmann constant,  $e$  is the typical charge in the plasma and  $\kappa_D$  is the inverse Debye length

$$\kappa_D \equiv \sqrt{4\pi\beta \sum_{\alpha} e_{\alpha}^2 \rho_{\alpha}^B} \quad (1.7)$$

where  $\rho_{\alpha}^B$  is the bulk value of the density for species with index  $\alpha$  (and  $e_{\alpha}$  is the charge of species  $\alpha$ ). The sum over  $\alpha$  runs from 1 to the number of species  $n_s$ . Every density profile takes the form

$$\rho_{\alpha}(x) = \rho_{\alpha}^B \theta(x-b) e^{-\beta e_{\alpha}^2 V_{\text{self}}^{\text{sc}}(x)} [1 - \beta e_{\alpha} \Phi(x)] \quad (1.8)$$

where  $V_{\text{self}}^{\text{sc}}(x)$  is a screened self-energy and  $\Phi(x)$  is the electrostatic potential created by the charge density profile  $\sum_{\gamma} e_{\gamma} \rho_{\gamma}(x)$ . ( $\Phi(x)$  is set to 0 in the

bulk.) The Heaviside function  $\theta(u)$ —with  $\theta(u) = 1$  if  $u > 0$  and  $\theta(u) = 0$  if  $u < 0$ —describes the geometric constraint enforced by the impenetrable wall. The analytic expressions are obtained in Section 3.  $\Phi(x)$ , given in (3.17), decays as  $\exp(-\kappa_D x)$  at large distances.  $V_{\text{self}}^{\text{sc}}(x)$  may be written as the sum

$$V_{\text{self}}^{\text{sc}}(x) = \frac{\kappa_D}{2} \bar{L}(\kappa_D x; \kappa_D b, \Delta_{\text{el}}) - \frac{\Delta_{\text{el}}}{4x} \exp(-2\kappa_D x) \quad (1.9)$$

$V_{\text{self}}^{\text{sc}}(x)$  falls off as  $\exp(-2\kappa_D x)/4x$  when  $x$  goes to infinity for all values of  $\Delta_{\text{el}}$ .  $(\kappa_D/2) \bar{L}$  given in (3.9) and (3.11) arises mainly from the geometric deformation of the screening cloud around a charge in the vicinity of the wall and remains finite at any distance. On the contrary,  $-e_\alpha^2(\Delta_{\text{el}}/4x) \times \exp(-2\kappa_D x)$  is the part of the screened self-energy originating from the bare self-energy  $e_\alpha^2 V_{\text{self}}^{\text{sc}}$  (1.5) due to the dielectric response of the wall. The second term in  $V_{\text{self}}^{\text{sc}}(x)$  was derived for the first time in the case  $\epsilon_w < 1$  from a phenomenological mean-field argument by Onsager and Samaras in 1934.<sup>(11)</sup> Its contribution to the density profile is crucial at short distances. When  $\epsilon_w < 1$  ( $\Delta_{\text{el}} < 0$ ) all charges are electrostatically repelled by the wall, the short-distance repulsion range  $b$  can be set to zero and the profile density vanishes exponentially fast at the contact ( $x = 0$ ) with the wall. On the contrary, when  $\epsilon_w > 1$  ( $\Delta_{\text{el}} > 0$ ), all charges are attracted by the wall,  $b$  must be kept finite and the contact value  $\rho_\alpha(b)$  increases as  $\exp[\Delta_{\text{el}} \beta e_\alpha^2 \exp(-2\kappa_D b)/(4b)]$  when  $b$  becomes small. In Section 3 we also derive the profile density in a OCP and we compare our result with that of ref. 1.

Section 4 is devoted to generic global properties of the plasma at the interface. In Section 5 we study the case of a plain hard wall ( $\epsilon_w = 1$ ). The analytic expressions are rather simple and we can investigate the only two effects which interplay: the geometric repulsion from the wall and the interaction with the electrostatic potential drop  $\Phi(x)$  created by the electric layer itself. In the case of a symmetric two-component plasma, we retrieve the results of ref. 8. In Section 6 the generic properties of the density profiles when  $\epsilon_w \neq 1$  are interpreted in terms of the competition between three effects: the two ones already at stake in the vicinity of a plain hard wall plus the electrostatic (repulsive or attractive) interaction due to the dielectric response of the wall. In particular, we exhibit how the structure of the charge density profile evolves from a double layer into a threefold layer and then into an inversed double layer when  $\epsilon_w$  increases from the value  $\epsilon_w = 1$ .

## 2. SELF-CONSISTENT SCHEME IN THE WEAK-COUPLING REGIME

### 2.1. Exact First BGY Equation

The exact density profile  $\rho_\alpha(x)$  is related to the Ursell function  $h_{\alpha\gamma}$  between species  $\alpha$  and  $\gamma$  through the first equation of the BGY hierarchy equation,

$$\begin{aligned} \frac{d}{dx} (\ln \rho_\alpha(x)) = & -\beta \frac{d}{dx} (e_\alpha \Phi(x) + e_\alpha^2 V_{\text{self}}(x)) \\ & - \beta e_\alpha \int d\mathbf{r}' \left( \sum_\gamma e_\gamma \rho_\gamma(x') h_{\alpha\gamma}(\mathbf{r}; \mathbf{r}') \right) \frac{\partial v_w}{\partial x}(\mathbf{r}'; \mathbf{r}) \end{aligned} \quad (2.1)$$

In (2.1)  $V_{\text{self}}(x)$  is the self-energy (1.4) due to the dielectric response of the wall, while  $\Phi(x)$  is the electrostatic potential created by the charge density profile  $\sum_\gamma e_\gamma \rho_\gamma(x)$ .  $\Phi(x)$  obeys Poisson equation

$$\Delta \Phi(x) = -4\pi \sum_\gamma e_\gamma \rho_\gamma(x) \quad (2.2)$$

$\Phi$  is uniform in the bulk, since a fundamental property of Coulomb systems is the local neutrality relation obeyed by the bulk densities

$$\sum_\alpha e_\alpha \rho_\alpha^{\text{B}} = 0 \quad (2.3)$$

for any value of the Coulomb coupling parameter. Thus, if we redefine  $\Phi(x)$  as the difference between the electrostatic potential created by the charge density and its bulk value,  $\Phi(x)$  tends to zero when  $x$  goes to  $+\infty$ .

We recall that, in the case  $\epsilon_w = 1$ , where there is no image forces, the density is merely uniform in the zero-coupling limit. In a plasma with no charge symmetry the potential drop  $\Phi(x)$ , which is determined from the charge density profile  $\sum_\gamma e_\gamma \rho_\gamma(x)$  through Poisson equation (2.2), does not vanish. Moreover, in the weak coupling regime, it is of the same order as the pair-correlation contribution to  $d\rho_\alpha/dx$  in the BGY equation, as shown *a posteriori* by our explicit calculations displayed in Section 3. By a mean-field scheme Guernsey<sup>(6)</sup> closed the second BGY equation in a weak-coupling limit and found that the zeroth-order pair correlation is calculated with uniform densities in a semi-infinite space. Thus he obtained coupled equations for  $d\rho_\alpha/dx$  and  $\Phi(x)$  and calculated  $\sum_\alpha e_\alpha \rho_\alpha(x)$  as a double integral. (The resolution was not performed for every  $\rho_\alpha(x)$  in the case  $\Phi(x) \neq 0$  though it might have been done.) The density profiles  $\rho_\alpha(x)$  were studied

only in the case of a symmetric two-component plasma. The first-order correction to their bulk value in the weak-coupling regime was calculated by Jancovici<sup>(8)</sup> as follows. Because of the charge symmetry specific to this system, the charge density profile and subsequently the electrostatic potential difference with the bulk  $\Phi(x)$  vanish at any distance from the wall. Then the gradient of the density  $\rho_\alpha(x)$  of species with charge  $e_\alpha$  given by the first BGY equation (2.1) is determined at leading order only by the zeroth-order pair correlation; the latter is calculated in a mean-field approximation for the direct correlation function with the same result as that found by Guernsey.<sup>(6)</sup>

When  $\epsilon_w \neq 1$  the methods introduced in the case  $\epsilon_w = 1$  cannot be generalized straightforwardly, because the fast variation of the density in the vicinity of the wall prevents one from using mere linearizations. In order to circumvent this difficulty we introduce the following scheme.

## 2.2. Mean-Field Ursell Function

In the first BGY equation (2.1)  $\sum_\gamma e_\gamma \rho_\gamma(x') h_{\alpha\gamma}(\mathbf{r}; \mathbf{r}')$  is the excess charge density of the screening cloud around a charge  $e_\alpha$  located at  $\mathbf{r}$ , the excess charge being calculated with respect to the charge density profile  $\sum_\gamma e_\gamma \rho_\gamma(x)$ . The electrostatic potential created at  $\mathbf{r}''$  by the charge  $e_\alpha$  and its screening cloud is

$$\Phi_{\text{exc}, \alpha}(\mathbf{r}; \mathbf{r}'') = e_\alpha v_w(\mathbf{r}; \mathbf{r}'') + \int d\mathbf{r}' \left( \sum_\gamma e_\gamma \rho_\gamma(x') h_{\alpha\gamma}(\mathbf{r}; \mathbf{r}') \right) v_w(\mathbf{r}'; \mathbf{r}'') \quad (2.4)$$

A mean-field approximation amounts to assuming that

$$\Phi_{\text{exc}, \alpha}^{MF}(\mathbf{r}; \mathbf{r}'') = e_\alpha \phi^{MF}(\mathbf{r}; \mathbf{r}'') \quad (2.5a)$$

$$h_{\alpha\gamma}^{MF}(\mathbf{r}; \mathbf{r}') = -\beta e_\alpha e_\gamma \phi^{MF}(\mathbf{r}; \mathbf{r}') \quad (2.5b)$$

(At leading order in the parameter  $\epsilon_D$ , the long-range Coulomb interaction prevails and the short-distance repulsion between particles is not involved in (2.5)). By inserting these approximations (2.5) into the definition (2.4), we obtain the well-known mean-field equation

$$\phi^{MF}(\mathbf{r}; \mathbf{r}'') = v_w(\mathbf{r}; \mathbf{r}'') - \beta \int d\mathbf{r}' \left( \sum_\gamma e_\gamma^2 \rho_\gamma(x') \right) v_w(\mathbf{r}; \mathbf{r}') \phi^{MF}(\mathbf{r}'; \mathbf{r}'') \quad (2.6)$$

Then the mean-field approximation of the integral in (2.1) proves to be equal to

$$-\frac{\beta e_\alpha^2}{2} \frac{\partial}{\partial x} [\phi^{MF} - v_w](\mathbf{r}; \mathbf{r}) \quad (2.7)$$

Indeed, the integral in (2.1) can be rewritten by means of the trick involving the Dirac distribution  $\delta(\mathbf{r} - \mathbf{r}'')$ ,

$$\int d\mathbf{r}' g(\mathbf{r}; \mathbf{r}') \frac{\partial f}{\partial x}(\mathbf{r}'; \mathbf{r}) = \int d\mathbf{r}'' \delta(\mathbf{r} - \mathbf{r}'') \frac{\partial}{\partial x} \left( \int d\mathbf{r}' g(\mathbf{r}''; \mathbf{r}') f(\mathbf{r}'; \mathbf{r}) \right) \quad (2.8)$$

Moreover, according to (1.1) and (2.6),  $\phi^{MF}(\mathbf{r}; \mathbf{r}')$  is the Green function of the operator  $\Delta_r - 4\pi\beta \sum_\gamma e_\gamma^2 \rho_\gamma(x')$ . Since the latter operator is self-adjoint, the real function  $\phi^{MF}(\mathbf{r}; \mathbf{r}')$ , as well as  $v_w(\mathbf{r}; \mathbf{r}')$ , is symmetric under exchange of  $\mathbf{r}$  and  $\mathbf{r}'$  when  $\mathbf{r}$  and  $\mathbf{r}'$  are in the same region. Then (2.6) can be used. Since a symmetric function  $h(\mathbf{r}; \mathbf{r}') = h(\mathbf{r}'; \mathbf{r})$  obeys the identity  $\partial[h(\mathbf{r}; \mathbf{r}')]/\partial x|_{\mathbf{r}=\mathbf{r}'} = (1/2) \partial[h(\mathbf{r}; \mathbf{r})]/\partial x$ , we get the result (2.7).

Finally, according to the definition (1.4) of  $V_{\text{self}}(x)$  and since  $\rho_\alpha(x)$  tends to  $\rho_\alpha^B$  when  $x$  goes to  $+\infty$ , the mean-field density profile  $\rho_\alpha^{MF}(x)$  proves to read

$$\rho_\alpha^{MF}(x) = \theta(x-b) \rho_\alpha^B \exp[-\beta e_\alpha^2 V_{\text{self}}^{sc}(x) - \beta e_\alpha \Phi^{MF}(x)] \quad (2.9)$$

with

$$V_{\text{self}}^{sc}(x) \equiv \frac{1}{2}(\phi^{MF} - v_B)(\mathbf{r}, \mathbf{r}) - \lim_{x \rightarrow +\infty} \frac{1}{2}(\phi^{MF} - v_B)(\mathbf{r}, \mathbf{r}) \quad (2.10)$$

Meanwhile the coupled equation for the electrostatic potential  $\Phi^{MF}(x)$  is (2.2) where  $\rho_\gamma(x)$  is replaced by  $\rho_\gamma^{MF}(x)$ . In (2.9) the argument in the exponential may be interpreted as  $\beta$  times the work given by an operator to the system in order to put a charge  $e_\alpha$  into the Coulomb fluid at  $\mathbf{r}$ , make it cross the potential drop  $\Phi^{MF}(x)$  from  $x$  to  $+\infty$  and then get it back from the bulk. In the following, we set

$$z_\alpha^{MF}(x) \equiv \theta(x-b) \rho_\alpha^B \exp[-\beta e_\alpha^2 V_{\text{self}}^{sc}(x)] \quad (2.11)$$

### 2.3. Linearization of the $\Phi(x)$ Contribution

Explicit calculations can be performed if the contribution from  $\Phi^{MF}(x)$  to

$$\rho_\alpha^{MF}(x) = z_\alpha^{MF}(x) e^{-\beta e_\alpha \Phi^{MF}(x)} \quad (2.12)$$

is linearized,

$$\rho_\alpha^{MF, \text{lin}}(x) = z_\alpha^{MF}(x)[1 - \beta e_\alpha \Phi^{MF, \text{lin}}(x)] \quad (2.13)$$

Such a linearization is allowed only if  $\Phi^{MF}(x)$  does not become infinite in the vicinity of the wall. This is indeed the case, because  $\Phi^{MF}(x)$  is created by the charge density and the latter has no singularity thanks to the hard-core repulsion from the wall. The absence of divergency in  $\Phi(x)$  near the wall is also checked in the systematic approach of Paper II. In the following we will show that the screened self-energy  $V_{\text{self}}^{sc}(x)$  diverges when  $x$  goes to zero and no linearization can be performed for it.

By inserting the linearized mean-field expression for the densities into Poisson equation (2.2) we find that

$$\left[ \Delta_r - 4\pi\beta \sum_\gamma e_\gamma^2 z_\gamma^{MF}(x) \right] \Phi^{MF, \text{lin}}(x) = -4\pi \sum_\gamma e_\gamma z_\gamma^{MF}(x) \quad (2.14)$$

(2.14) can be viewed as some kind of partially linearized Poisson–Boltzmann equation in an inhomogeneous case. As a consequence of (2.14),

$$\Phi^{MF, \text{lin}}(x) = \int d\mathbf{r}' \phi_z^{MF, \text{lin}}(\mathbf{r}', \mathbf{r}) \sum_\gamma e_\gamma z_\gamma^{MF}(x') \quad (2.15)$$

where  $\phi_z^{MF, \text{lin}}(\mathbf{r}, \mathbf{r}')$  is a Green function solution of

$$[\Delta_r - \kappa_D^2(1 + U(\mathbf{r}))] \phi_z^{MF, \text{lin}}(\mathbf{r}, \mathbf{r}') = -4\pi\delta(\mathbf{r} - \mathbf{r}') \quad (2.16)$$

with

$$U(\mathbf{r}) = \frac{4\pi\beta}{\kappa_D^2} \sum_\gamma e_\gamma^2 [z_\gamma^{MF}(x) - \rho_\gamma^B] \quad (2.17)$$

$\phi_z^{MF, \text{lin}}$  is the solution of (2.16) which satisfies the same boundary conditions as  $v_w(\mathbf{r}, \mathbf{r}')$ .

## 2.4. Solution of the Inhomogeneous Debye–Hückel Equation at Leading Order

A formal solution of the inhomogeneous Debye–Hückel equation (2.16) is given in Paper II. An  $\varepsilon_D$ -expansion is devised and we show that

$$\phi_z^{MF, \text{lin}}(\mathbf{r}, \mathbf{r}') = \kappa_D \tilde{\phi}^{(0)}(\kappa_D \mathbf{r}, \kappa_D \mathbf{r}') [1 + \mathcal{O}_{\text{exp}}(\varepsilon_D)] \quad (2.18)$$

In (2.18)  $\mathcal{O}_{\text{exp}}(\varepsilon_D)$  denotes a function of order  $\varepsilon_D$ —possibly multiplied by some power of  $\ln \varepsilon_D$ —which decays exponentially fast at large distances over a scale  $\kappa_D^{-1}$  and which remains bounded by a function of  $\beta e^2/b$  for all  $x$  larger than the closest approach distance  $b$  to the wall.  $\kappa_D \tilde{\phi}^{(0)}$  is the solution of the homogeneous Debye–Hückel equation

$$[A_r - \kappa_D^2] \kappa_D \tilde{\phi}^{(0)}(\kappa_D \mathbf{r}, \kappa_D \mathbf{r}') = -4\pi\delta(\mathbf{r} - \mathbf{r}') \quad (2.19)$$

with the same electrostatic boundary conditions as  $v_w(\mathbf{r}, \mathbf{r}')$ :  $\tilde{\phi}^{(0)}$  is continuous in all space and

$$\lim_{x \rightarrow 0^-} \epsilon_w \frac{\partial \tilde{\phi}^{(0)}}{\partial x}(\kappa_D \mathbf{r}, \kappa_D \mathbf{r}') = \lim_{x \rightarrow 0^+} \frac{\partial \tilde{\phi}^{(0)}}{\partial x}(\kappa_D \mathbf{r}, \kappa_D \mathbf{r}') \quad (2.20)$$

Equation (2.18) also holds for  $\phi^{MF}$  defined in (2.6) and which obeys equation (2.16) where  $z_\gamma^{MF}(x)$  in  $U(\mathbf{r})$  is replaced by  $\rho_\gamma(x)$ . Thus the screened self-energy defined in (2.10) is also determined at leading order in  $\varepsilon_D$ .

Eventually, the density profile at leading order in  $\varepsilon_D$  is given by (2.11) and (2.13) with

$$V_{\text{self}}^{sc}(x) = \frac{1}{2} \kappa_D [\tilde{\phi}^{(0)} - \tilde{\phi}_B](\kappa_D \mathbf{r}, \kappa_D \mathbf{r}) \quad (2.21)$$

and

$$\Phi^{MF, \text{lin}}(x) = \int d\mathbf{r}' \kappa_D \tilde{\phi}^{(0)}(\kappa_D \mathbf{r}, \kappa_D \mathbf{r}') \sum_\gamma e_\gamma z_\gamma^{MF}(x') \quad (2.22)$$

In (2.21)  $\tilde{\phi}_B$  denotes the solution of the homogeneous Debye–Hückel equation in the bulk, namely the solution which vanishes when  $|\mathbf{r} - \mathbf{r}'|$  becomes infinite, as well as  $v_B(\mathbf{r}, \mathbf{r}')$  defined in (1.3).

### 3. EXPLICIT DENSITY PROFILES

#### 3.1. Solution of the Homogeneous Debye Equation

Equation (2.19) can be solved because it is changed into a second-order differential equation by taking the Fourier transform in the direction parallel to the wall,

$$\tilde{\phi}^{(0)}(\tilde{x}, \tilde{x}', \mathbf{q}) = \int d\tilde{\mathbf{y}} e^{i\mathbf{q} \cdot \tilde{\mathbf{y}}} \tilde{\phi}^{(0)}(\tilde{x}, \tilde{x}', \tilde{\mathbf{y}}) \quad (3.1)$$

In (3.1) we have used the dimensionless variables  $\tilde{x} = \kappa_D x$  and  $\tilde{y} = \kappa_D y$ , where  $y$  is the projection of  $\mathbf{r}$  onto a plane parallel to the wall. As recalled in Paper II, since  $\kappa_D \tilde{\phi}^{(0)}$  obeys the same boundary conditions as  $v_w$ , for  $x > b$  and  $x' > b$

$$\tilde{\phi}^{(0)}(\tilde{x}, \tilde{x}', \mathbf{q}; \tilde{b}, \Delta_{\text{el}}) = \tilde{\phi}_{\text{B}}(|\tilde{x} - \tilde{x}'|, \mathbf{q}) + Z(\mathbf{q}; \tilde{b}, \Delta_{\text{el}}) \tilde{h}_{\text{HW}}^+(\tilde{x} + \tilde{x}' - 2\tilde{b}; \mathbf{q}) \quad (3.2)$$

with

$$\tilde{\phi}_{\text{B}}(|\tilde{x} - \tilde{x}'|, \mathbf{q}) = \frac{2\pi}{\sqrt{1+q^2}} e^{-|\tilde{x} - \tilde{x}'| \sqrt{1+q^2}} \quad (3.3)$$

$$\tilde{h}_{\text{HW}}^+(\tilde{x} + \tilde{x}' - 2\tilde{b}; \mathbf{q}) = \frac{2\pi}{\sqrt{1+q^2}} \frac{\sqrt{1+q^2} - |\mathbf{q}|}{\sqrt{1+q^2} + |\mathbf{q}|} e^{-(\tilde{x} + \tilde{x}' - 2\tilde{b}) \sqrt{1+q^2}} \quad (3.4)$$

and

$$Z(\mathbf{q}; \tilde{b}, \Delta_{\text{el}}) \equiv \frac{1 - \Delta_{\text{el}} e^{-2q\tilde{b}} [\sqrt{1+q^2} + |\mathbf{q}|]^2}{1 - \Delta_{\text{el}} e^{-2q\tilde{b}} [\sqrt{1+q^2} - |\mathbf{q}|]^2} \quad (3.5)$$

### 3.2. Screened Self-Energy

The screened self-energy (2.21) can be written as

$$\beta e_\alpha^2 V_{\text{self}}^{\text{sc}}(x) = \varepsilon_\alpha L(\tilde{x} - \tilde{b}; \tilde{b}, \Delta_{\text{el}}) \quad (3.6)$$

with  $\varepsilon_\alpha \equiv (1/2) \beta e_\alpha^2 \kappa_D$  and

$$L(\tilde{x} - \tilde{b}; \tilde{b}, \Delta_{\text{el}}) \equiv \int \frac{d^2 \mathbf{q}}{(2\pi)^2} [\tilde{\phi}^{(0)}(\tilde{x}, \tilde{x}, \mathbf{q}; \tilde{b}, \Delta_{\text{el}}) - \tilde{\phi}_{\text{B}}(\tilde{x}, \tilde{x}, \mathbf{q})] \quad (3.7)$$

According to (3.2)

$$L(u; \tilde{b}, \Delta_{\text{el}}) = \int \frac{d^2 \mathbf{q}}{(2\pi)^2} Z(\mathbf{q}; \tilde{b}, \Delta_{\text{el}}) \times \tilde{h}_{\text{HW}}^+(2u; \mathbf{q}) \quad (3.8)$$

where  $\tilde{h}_{\text{HW}}^+$  is given in (3.4). By using the change of variable  $t = \sqrt{1+q^2}$  we get

$$L(\tilde{x} - \tilde{b}; \tilde{b}, \Delta_{\text{el}}) = \int_1^{+\infty} dt \frac{1 - \Delta_{\text{el}} [t + \sqrt{t^2 - 1}]^2 e^{-2\tilde{b} \sqrt{t^2 - 1}}}{[t + \sqrt{t^2 - 1}]^2 - \Delta_{\text{el}} e^{-2\tilde{b} \sqrt{t^2 - 1}}} e^{-2(\tilde{x} - \tilde{b})t} \quad (3.9)$$

The successive changes of variables  $t = t' + 1$  then  $t' = v/[2(\tilde{x} - \tilde{b})]$  allow to show that

$$L(\tilde{x} - \tilde{b}; \tilde{b}, \Delta_{el}) \underset{\tilde{x} \rightarrow +\infty}{\sim} \frac{e^{-2(\tilde{x} - \tilde{b})}}{2(\tilde{x} - \tilde{b})} \quad (3.10)$$

If  $\tilde{b} \neq 0$  the integrand in (3.9) behaves as  $1/t^2$  times  $\exp[-2(\tilde{x} - \tilde{b})t]$  when  $t$  goes to  $+\infty$  and  $L(\tilde{x} - \tilde{b}, \tilde{b}, \Delta_{el})$  is finite for all values of  $\tilde{x}$  even when  $\tilde{x}$  approaches  $\tilde{b}$ . If  $\tilde{b} = 0$  the integrand vanishes as  $\exp(-2\tilde{x}t)/t^2$  for large  $t$  when  $\Delta_{el} = 0$  but it behaves as  $-\Delta_{el} \exp(-2\tilde{x}t)$  if  $\Delta_{el} \neq 0$ . Subsequently for  $\tilde{b} = 0$ , the integral diverges at  $\tilde{x} = \tilde{b} = 0$  when  $\Delta_{el} \neq 0$ . By subtracting the dangerous asymptotic behaviour  $I_{as}(t) = -\Delta_{el} \exp[-2\tilde{x}t]$  from the integrand of  $L$  and by performing  $\int_1^{+\infty} dt I_{as}(t)$  we get

$$L(\tilde{x} - \tilde{b}; \tilde{b}, \Delta_{el}) = -\Delta_{el} \frac{e^{-2\tilde{x}}}{2\tilde{x}} + \bar{L}(\tilde{x}; \tilde{b}, \Delta_{el}) \quad (3.11)$$

where  $\bar{L}(\tilde{x}; \tilde{b}, \Delta_{el})$  remains finite even when  $\tilde{x} = \tilde{b} = 0$ .

### 3.3. Electrostatic Potential Drop

In order to calculate the electrostatic potential drop (2.22), we notice that

$$\tilde{\phi}^{(0)}(\tilde{x}, \tilde{x}', \mathbf{q} = \mathbf{0}; \tilde{b}) = 2\pi[e^{-|\tilde{x} - \tilde{x}'|} + e^{-(\tilde{x} + \tilde{x}' - 2\tilde{b})}] \quad (3.12)$$

and we rewrite  $z_\alpha^{MF}(x)$  as

$$z_\alpha^{MF}(x) = \rho_\alpha^B [1 + w_0(\tilde{x}; \varepsilon_\alpha, \Delta_{el})][1 - \varepsilon_\alpha \bar{L}(\tilde{x}; \tilde{b}, \Delta_{el})] \quad (3.13)$$

with

$$w_0(\tilde{x}; \varepsilon_\alpha, \Delta_{el}) \equiv \exp \left[ \Delta_{el} \frac{\beta e_\alpha^2}{4x} e^{-2\kappa_D x} \right] - 1 \quad (3.14)$$

According to the bulk neutrality relation (2.3), the constant term in  $z_\alpha^{MF}(x)$  gives a vanishing contribution to (2.22).  $w_0(\tilde{x}; \varepsilon_\alpha, \Delta_{el})$  proves to contribute from order  $\varepsilon_D \ln \varepsilon_D$  to the integral in (2.22). Indeed, let us consider a function  $f(\tilde{x}'; \tilde{x}, \tilde{b})$  which is bounded for all  $\tilde{x}' \geq 0$  and  $\tilde{b} \geq 0$ . If  $b > \kappa_D^{-1}$ , then for all  $x > b$   $\beta e_\alpha^2/x < \kappa_D \beta e_\alpha^2$  and

$$\kappa_D \int_b^{+\infty} dx' w_0(\tilde{x}'; \varepsilon_\alpha, \Delta_{el}) f(\tilde{x}'; \tilde{x}, \tilde{b}) \underset{\varepsilon_\alpha \rightarrow 0}{\sim} \kappa_D \int_{\tilde{b}}^{+\infty} d\tilde{x}' \frac{\Delta_{el} \beta e_\alpha^2}{4\tilde{x}'} e^{-2\tilde{x}'} f(\tilde{x}'; \tilde{x}, \tilde{b}) \quad (3.15)$$

In the case  $b \ll \kappa_D^{-1}$ , let us introduce the length  $l$  such that  $\beta e_\alpha^2 \ll l \ll \kappa_D^{-1}$ . For all  $x$  in the range  $b < x < l$ ,  $\kappa_D x \ll 1$ , while, for all  $x > l$ ,  $\beta e_\alpha^2/x \ll 1$ . Then at leading order in  $\varepsilon_D$

$$\begin{aligned} &\kappa_D \int_b^{+\infty} dx' w_0(\tilde{x}'; \varepsilon_\alpha, \Delta_{el}) f(\tilde{x}'; \tilde{x}, \tilde{b}) \\ &\sim \lim_{\varepsilon_\alpha \rightarrow 0} \lim_{l/\beta e_\alpha^2 \rightarrow +\infty} \lim_{\kappa_D l \rightarrow 0} \left\{ \kappa_D \int_b^l dx' \left[ \exp\left(\frac{\Delta_{el} \beta e_\alpha^2}{4x'}\right) - 1 \right] f(\tilde{x}' = 0; \tilde{x}, \tilde{b} = 0) \right. \\ &\quad \left. + \kappa_D \int_l^{+\infty} d\tilde{x}' \frac{\Delta_{el} \beta e_\alpha^2}{4\tilde{x}'} e^{-2\tilde{x}'} f(\tilde{x}'; \tilde{x}, \tilde{b} = 0) \right\} \times [1 + \mathcal{O}(\tilde{b})] \end{aligned} \quad (3.16)$$

where  $\mathcal{O}(\tilde{b})$  denotes a term of order  $\tilde{b}$ . After the change of variable  $x' = x'_1 \beta e_\alpha^2$ , the first integral in (3.16) proves to be of order  $\varepsilon_\alpha$ , as well as the second integral. Both integrals have a logarithmic dependence upon  $l$  and the respective  $\ln(l/\beta e_\alpha^2)$  and  $\ln(\kappa_D l)$  terms combine so that the sum of the two integrals starts at order  $\varepsilon_D \ln \varepsilon_D$ .

Eventually, we get for  $\Phi^{MF, \text{lin}}(x)$ , denoted by  $\Phi(x)$  in the following,

$$\Phi(x) = -\frac{2\pi\beta}{\kappa_D} \sum_\gamma \rho_\gamma e_\gamma^3 M_\gamma(\kappa_D x; \varepsilon_\gamma, \kappa_D b, \Delta_{el}) \times [1 + \mathcal{O}_{\text{exp}}(\varepsilon_D)] \quad (3.17)$$

where  $\mathcal{O}_{\text{exp}}(\varepsilon_D)$  is defined after (2.18). In (3.17)  $M_\gamma = \bar{M} + [M_\gamma - \bar{M}]$  with

$$\bar{M}(\tilde{x}; \tilde{b}, \Delta_{el}) = \frac{1}{2} \int_{\tilde{b}}^{+\infty} du' [e^{-|\tilde{x}-u'|} + e^{-(\tilde{x}+u'-2\tilde{b})}] \bar{L}(u'; \tilde{b}, \Delta_{el}) \quad (3.18)$$

and  $M_\gamma - \bar{M}$  is the  $\varepsilon_D$ -expansion at orders  $\ln \varepsilon_\gamma$  and  $(\varepsilon_\gamma)^0$  of the integral

$$-\frac{1}{2} \frac{1}{\varepsilon_\gamma} \int_{\tilde{b}}^{+\infty} du' [e^{-|\tilde{x}-u'|} + e^{-(\tilde{x}+u'-2\tilde{b})}] w_0(u'; \varepsilon_\gamma, \Delta_{el}) \quad (3.19)$$

### 3.4. Density Profile

The previous expressions are inserted in (2.13) with the result

$$\begin{aligned} \rho_\alpha(x) = &\rho_\alpha^B \theta(x-b) \exp\left(\Delta_{el} \frac{\beta e_\alpha^2}{4x} e^{-2\kappa_D x}\right) \times \left\{ 1 - \frac{1}{2} \beta \kappa_D \left[ e_\alpha^2 \bar{L}(\kappa_D x; \kappa_D b, \Delta_{el}) \right. \right. \\ &\left. \left. - e_\alpha \frac{4\pi\beta}{\kappa_D^2} \sum_\gamma \rho_\gamma^B e_\gamma^3 M_\gamma(\kappa_D x; \varepsilon_\gamma, \kappa_D b, \Delta_{el}) \right] \right\} \end{aligned} \quad (3.20)$$

where  $\varepsilon_\gamma = (1/2) \beta e_\gamma^2 \kappa_D$ .  $M_\gamma$  is defined in (3.18) and (3.19), while  $\bar{L}$  is given by (3.9) and (3.11).  $\bar{L}(\tilde{x}; \tilde{b}, \Delta_{\text{el}})$  decreases exponentially fast as  $\exp(-2\tilde{x})/2\tilde{x}$  when  $\tilde{x}$  goes to  $\infty$ , while  $M_\gamma$  decays only as  $\exp(-\tilde{x})/\tilde{x}$ .

We give more explicit formulae in the regime

$$\eta \equiv \kappa_D b \ll 1 \quad (3.21)$$

whatever the value of  $\beta e^2/b$  may be. When  $\varepsilon_D \ll 1$ , according to (1.6) and (1.7), the mean interparticle distance  $a$  is smaller than  $\kappa_D^{-1}$ ,  $a < \kappa_D^{-1}$  and the condition (3.21) will be fulfilled if  $b \ll a$ —for instance if  $b$  is of the same magnitude as the hard-core diameter of charges which itself is far smaller than  $a$ .  $\bar{L}(\tilde{x}; \kappa_D b, \Delta_{\text{el}})$  is bounded for every  $x$ , even when  $\eta = \kappa_D b$  vanishes, and it can be expanded in powers of  $\eta$ . According to (3.9) and (3.11),  $\bar{L}(\tilde{x}; \eta = 0, \Delta_{\text{el}})$  is directly given by

$$\bar{L}(\tilde{x}; \eta = 0, \Delta_{\text{el}}) = \int_1^{+\infty} dt e^{-2t\tilde{x}} \frac{(1 - \Delta_{\text{el}}^2)}{(t + \sqrt{t^2 - 1})^2 - \Delta_{\text{el}}} \quad (3.22)$$

On the other hand

$$\begin{aligned} M_\gamma(\tilde{x}; \varepsilon_\gamma, \eta = 0, \Delta_{\text{el}}) \\ = \bar{M}(\tilde{x}; \eta = 0, \Delta_{\text{el}}) + (\ln \varepsilon_\gamma) \Delta_{\text{el}}^{1/2} e^{-\tilde{x}} - \Delta_{\text{el}} I_\gamma(\tilde{x}; \Delta_{\text{el}}, \beta e_\gamma^2/b) \end{aligned} \quad (3.23)$$

where

$$\bar{M}(\tilde{x}; \eta = 0, \Delta_{\text{el}}) = \int_1^{+\infty} dt \left[ \frac{e^{-2t\tilde{x}} - 2te^{-\tilde{x}}}{1 - (2t)^2} \right] \frac{1 - \Delta_{\text{el}}^2}{(t + \sqrt{t^2 - 1})^2 - \Delta_{\text{el}}} \quad (3.24)$$

while, according to (3.16),

$$\begin{aligned} I_\gamma(\tilde{x}; \Delta_{\text{el}}, \beta e_\gamma^2/b) = -\frac{1}{4} e^{-\tilde{x}} \left\{ 2 \left[ A \left( \frac{\beta e_\gamma^2 \Delta_{\text{el}}}{4b} \right) + \ln \left( \frac{|\Delta_{\text{el}}|}{2} \right) + 2C - 1 \right] + \ln 3 \right\} \\ + \frac{1}{4} e^{-2\tilde{x}} [e^{\tilde{x}} \text{Ei}(-\tilde{x}) - e^{3\tilde{x}} \text{Ei}(-3\tilde{x})] \end{aligned} \quad (3.25)$$

In (3.25)  $C$  is the Euler constant,  $\text{Ei}(-u)$  denotes the Exponential-Integral function defined for  $u > 0$  as  $\text{Ei}(-u) \equiv -\int_u^{+\infty} dt \exp(-t)/t$

$$A(u) \equiv \frac{1}{u} [e^u - 1] - \text{Ei}(u) \quad (3.26)$$

$A(u)$  arises from the integration of  $\exp(-\beta e_\gamma^2 \Delta_{\text{el}}/4u) - 1$  in (3.19).

### 3.5. Interpretation: Competition Between Three Effects

The profile density is ruled by the competition between three kinds of effective interactions, as exhibited by rewriting the density profile by means of (2.9), (3.6) and (3.11) with the result

$$\rho_\alpha(x) = \rho_\alpha^B e^{\Delta_{el} \beta e_\alpha^2 (e^{-2\kappa_D x}/4x)} \times \left\{ 1 - \beta e_\alpha^2 \frac{\kappa_D}{2} \bar{L}(\kappa_D x; \kappa_D b, \Delta_{el}) - \beta e_\alpha \Phi(x) + \mathcal{O}_{\text{exp}}(\varepsilon_D^2) \right\} \quad (3.27)$$

where  $\mathcal{O}_{\text{exp}}(\varepsilon_D^2)$  is defined after (2.18). The interpretation of (3.27) is the following.

First,  $e_\alpha \Phi(x)$  is the interaction between a charge  $e_\alpha$  and the charge profile density in the electric layer. The other two interactions, which are proportional to  $e_\alpha^2$ , are the two parts of the screened self-energy.

Second,  $\exp(\Delta_{el} \beta e_\alpha^2 \exp(-2\kappa_D x)/4x)$  is the effective Boltzmann factor associated with the part of the screened self-energy created by the electrostatic response of the wall. The effect of the corresponding attractive ( $\Delta_{el} > 0$ ) or repulsive ( $\Delta_{el} < 0$ ) interaction with the wall cannot be linearized. Indeed, when the dielectric wall is repulsive, the density vanishes as  $\exp(-|\Delta_{el}| \beta e_\alpha^2/4b)$  when  $b$  goes to zero. Since the hard-core repulsion is spurious when  $\Delta_{el} < 0$ , we can set  $b = 0$  and

$$\rho_\alpha(x=0, \Delta_{el} < 0) = 0 \quad (3.28)$$

On the contrary when  $\Delta_{el} > 0$ , the density blows up as

$$\rho_\alpha(x=b, \Delta_{el}) \underset{b \rightarrow 0}{\sim} \rho_\alpha^B \exp \left\{ \frac{\Delta_{el} \beta e_\alpha^2 e^{-\kappa_D b}}{4b} \right\} [1 + \mathcal{O}(\varepsilon_D)] \quad (3.29)$$

Third, the part of the screened self-energy which exists even in the absence of any electrostatic property of the wall (namely even when  $\Delta_{el} = 0$ ) is  $(\kappa_D/2) \bar{L}(\kappa_D x; \kappa_D b, \Delta_{el})$ ; it arises from the “geometric” repulsion caused by the mere presence of the wall. Indeed, by deforming the screening cloud (with a net charge  $-e_\alpha$ ) surrounding any charge  $e_\alpha$ , the wall hinders the stabilizing effect of Coulomb interactions, as exhibited clearly in Section 5.3 about the plain hard wall.

### 3.6. Limiting Case of the OCP

The density profile for a one-component plasma (OCP) can be derived from the expression obtained for a two-component plasma by the following

trick already tested in refs. 2 and 4. In order to describe a OCP where moving particles carry a positive charge  $e$  in a neutralizing uniform background with density  $\rho$ , we start from a two-component plasma with  $e_+ = e$  and  $\rho_+ = \rho$  and we take the limit where  $e_-/e_+$  vanishes while  $e_-\rho_- = -e_+\rho_+$  is kept fixed.

The general expression (3.20) tends to the limit

$$\rho_{\text{OCP}} = \rho\theta(x-b) \exp\left[\frac{\Delta_{\text{el}}\beta e^2 e^{-2\kappa_D x}}{4x}\right] \times \left\{1 - \frac{1}{2}\beta\kappa_D e^2 [\bar{L}(\kappa_D x; \kappa_D b, \Delta_{\text{el}}) - M_{\text{OCP}}(\kappa_D x; \beta\kappa_D e^2/2, \kappa_D b, \Delta_{\text{el}})]\right\} \quad (3.30)$$

where  $\kappa_D = \sqrt{4\pi\beta\rho e^2}$ ,  $\bar{L}$  is defined by (3.9) and (3.11), while  $M_{\text{OCP}}$  is equal to the function  $M_\gamma$  defined in (3.18) and (3.19) with  $\varepsilon_\gamma$  replaced by  $\kappa_D\beta e^2/2$ . According to (3.17), the potential difference with the bulk is

$$\Phi_{\text{OCP}}(x) = -\frac{1}{2}\kappa_D e M_{\text{OCP}}(\kappa_D x; \beta\kappa_D e^2/2, \kappa_D b, \Delta_{\text{el}}) \quad (3.31)$$

We recall that (3.30) can also be rewritten as

$$\rho_{\text{OCP}}(x) = \rho\theta(x-b) e^{-\beta e^2 V_{\text{self}}^{\text{sc}}(x)} [1 - \beta e \Phi_{\text{OCP}}(x)] \quad (3.32)$$

where  $V_{\text{self}}^{\text{sc}}(x)$  is given in (1.9). Moreover, according to (3.12), (2.22) may be rewritten in the case of the OCP as

$$\begin{aligned} \frac{1}{2} \int_b^{+\infty} d\tilde{x}' [e^{-\beta e^2 V_{\text{self}}^{\text{sc}}(\tilde{x}')} - 1] [e^{-|\tilde{x} - \tilde{x}'|} + e^{-(\tilde{x} + \tilde{x}' - 2b)}] \\ = \beta e \Phi_{\text{OCP}}(x; \tilde{b}) + \mathcal{O}_{\text{exp}}(\varepsilon_D^2) \end{aligned} \quad (3.33)$$

### 3.7. Comparison with Previous Results

The expression (3.30) for the OCP is valid at any distance from the wall and for any value of  $\Delta_{\text{el}}$  and  $\kappa_D b$ . Let us see how it can be compared with the expression (3.21) in ref. 1 obtained in the case  $\Delta_{\text{el}} < 0$  and  $b = 0$ , and for distances  $x \gg \beta e^2$ . (The expressions in ref. 1 will be denoted by a superscript \*.)

Alastuey starts from the BGY equation (2.1) and directly replaces the Ursell function by its Debye approximation  $-\beta e^2 \kappa_D \tilde{\phi}^{(0)}(\kappa_D \mathbf{r}, \kappa_D \mathbf{r}'; \Delta_{\text{el}})$ . The equation (3.17) in ref. 1—which is analogous to our equation

(2.14)—involves the screened self-energy calculated at leading order in  $\varepsilon_D$ —as in the present paper—and given by

$$V_{\text{self}}^{\text{sc}*}(x) = \varepsilon_D L(\kappa_D x; \Delta_{\text{el}}) \quad (3.34)$$

However the equation (3.17) in ref. 1 is solved only for distances  $x \gg \beta e^2$  which are large enough to allow one to replace  $U(\mathbf{r})$ , defined in our equation (2.17), by zero. The corresponding approximated  $\Phi_{\text{OCP}}^*$  is solution of

$$\left[ \frac{d^2}{dx^2} - \kappa_D^2 \right] \Phi_{\text{OCP}}^*(x) = -\frac{\kappa_D^2}{\beta e} e^{-\beta e^2 V_{\text{self}}^{\text{sc}*}(x)} \quad x \gg \beta e^2 \quad (3.35)$$

while, according to the Poisson equation which relates  $d^2\Phi_{\text{OCP}}^*/dx^2$  and the charge density  $e[\rho(x) - \rho]$ ,

$$\rho_{\text{OCP}}^*(x) = \rho [e^{-\beta e^2 V_{\text{self}}^{\text{sc}*}(x)} - \beta e \Phi_{\text{OCP}}^*(x)] \quad x \gg \beta e^2 \quad (3.36)$$

((3.36) is the formula (3.21) given in ref. 1.) According to the result (2.18) of our analysis of the non approximated equation (2.16) (see Paper II), the expression of  $\Phi_{\text{OCP}}^*$ , solution of (3.35) and given in Eq. (3.20) of ref. 1, coincides with our formula (3.33) valid at any distance. On the other hand, the result (3.36) does coincide with the  $x \gg \beta e^2$  limit of the expression (3.32) which is valid for any  $x$ .

Our ability to handle with all distances relies on two progresses with respect to the approach of ref. 1. First, we extract from the expression of  $e_\alpha^2 V_{\text{self}}^{\text{sc}*}(x)$  the part which diverges as the bare self-energy  $\Delta_{\text{el}} e_\alpha^2 / (4x)$  when  $x$  approaches the wall and which enforces the vanishing of the density at the wall when  $b = 0$ . Second, we are able to disentangle this short-range effect from the long-range exponential screening through our systematic method of expansion introduced in Paper II for the solutions of the inhomogeneous Debye–Hückel equations at stake.

## 4. GENERIC GLOBAL PROPERTIES

### 4.1. Potential Drop

First we recall that in the generic case the local neutrality valid in the bulk is destroyed near the wall,

$$\sum_{\alpha} e_{\alpha} \rho_{\alpha}(x) \neq 0 \quad (4.1)$$

and there appears an electric layer which is responsible for a potential drop  $\Phi(x)$  between each point and the bulk. The expression of  $\Phi(x)$  is given in (3.17).  $\bar{M}$  in the decomposition of  $M_\gamma$  is a positive function, whereas  $M_\gamma - \bar{M}$  may have any sign. Thus the profile of  $\Phi$  depends on the composition  $\{e_\gamma, \rho_\gamma\}_{\gamma=1, \dots, n_s}$  of the Coulomb fluid and on the value of  $\Delta_{el}$ . For instance, when  $\kappa_D b \ll 1$ ,

$$\Phi(x=0) = -\frac{2\pi\beta}{\kappa_D} \sum_\gamma \rho_\gamma^B e_\gamma^3 \left\{ (1 - \Delta_{el}^2) J(\Delta_{el}) + \frac{\Delta_{el}}{2} \left[ \ln \left( 3\kappa_D \beta e_\gamma^2 |\Delta_{el}|/4 \right) - 1 + 2C + A \left( \frac{\Delta_{el} \beta e_\gamma^2}{4b} \right) \right] + \mathcal{O}(\varepsilon_D; \kappa_D b) \right\} \tag{4.2}$$

In (4.2)  $\mathcal{O}(\varepsilon_D; \kappa_D b)$  denotes a term of order either  $\varepsilon_D$  or  $\kappa_D b$ , and

$$J(\Delta_{el}) = \frac{1}{4(1 + \Delta_{el} + \Delta_{el}^2)} \left\{ -\frac{\pi}{\sqrt{3}} + (1 + 2\Delta_{el}) \ln 3 + \frac{1 - \Delta_{el}^2}{\Delta_{el}} \ln(1 - \Delta_{el}) + \frac{1 - \Delta_{el}}{\sqrt{\Delta_{el}}} \ln \left( \frac{1 + \sqrt{\Delta_{el}}}{1 - \sqrt{\Delta_{el}}} \right) \right\} \tag{4.3}$$

An example for the profile  $\Phi(x)$  is drawn in Fig. 1.

However the local neutrality  $\sum_\alpha e_\alpha \rho_\alpha(x) = 0$  holds in the specific case of a charge-symmetric plasma in a symmetric state, for any strength of the

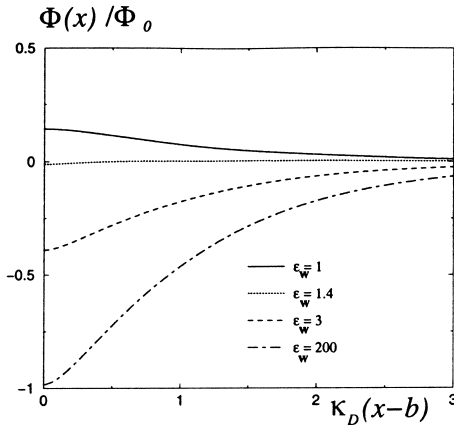


Fig. 1. Profile of the electrostatic potential  $\Phi(x)$  for  $\kappa_D b = 0.1$  in the limit  $\Delta_{el} \beta e^2/b \ll 1$ .  $M_\gamma$  in (3.23) does no longer depend on  $\gamma$  in the limit  $\Delta_{el} \beta e^2/b \ll 1$ .  $\Phi_0 = -\sum_\gamma \beta e_\gamma^3 \rho_\gamma^B / \kappa_D$ . The values of  $\varepsilon_w$  are displayed in the figure.

Coulomb coupling in the fluid. We use the following definitions. A charge-symmetric fluid contains equal numbers of positively and negatively charged species and the set of charges is invariant under inversion of charges. In the special case of a two-component plasma made of charges  $+e$  and  $-e$ , the latter charge symmetry combined with the neutrality relation (2.3) implies that  $\rho_+^B = \rho_-^B$ . On the contrary, for a charge-symmetric plasma with at least four species  $\rho_\alpha^B \neq \rho_{-\alpha}^B$  in the generic case. However, in some situations (for instance when two different salts made with monovalent ions are dissolved in water) the system is prepared in a symmetric state; the bulk density parameters are chosen to satisfy

$$\rho_\alpha^{B \text{ sym}} = \rho_{-\alpha}^{B \text{ sym}} \quad (4.4)$$

In such a symmetric state, the symmetry of the Hamiltonian under inversion of charge signs enforces that at any point  $x$

$$\sum_\alpha e_\alpha \rho_\alpha^{\text{sym}}(x) = 0 \quad (4.5)$$

and, subsequently

$$\Phi^{\text{sym}}(x) = 0 \quad (4.6)$$

In a symmetric state, a charge-symmetric Coulomb fluid does not build any charge density profile or any electrostatic potential difference with the bulk.

## 4.2. Global Charge

A dielectric wall remains globally neutral in the presence of a Coulombic fluid and may only acquire macroscopic multipoles depending on the geometry of the dielectric sample. As a consequence, we expect<sup>(10)</sup> that, since  $\epsilon_w < +\infty$ ,

$$\int_0^{+\infty} dx \sum_\alpha e_\alpha \rho_\alpha(x) = 0 \quad (4.7)$$

We recall that  $\Phi(x=0) \neq 0$  means that the dielectric layer carries a non-vanishing dipole though its net charge is zero.

The global charge of the system calculated at leading order  $\epsilon_D$  indeed vanishes in agreement with (4.7). The result is readily obtained by writing for  $\rho_\alpha(x)$  the structure (2.13) combined with (2.22) and by using the

following property. According to (3.15) and (3.16), if  $f(x)$  is an integrable function which is bounded for every  $x \geq 0$ ,

$$\int_0^{+\infty} dx z_\alpha^{MF}(x) f(x) = \rho_\alpha^B \int_0^{+\infty} dx f(x) \times [1 + \mathcal{O}(\varepsilon_D \ln \varepsilon_D)] \quad (4.8)$$

Eqs. (2.13) and (4.8) lead to

$$\begin{aligned} \int_0^{+\infty} dx \sum_\alpha e_\alpha \rho_\alpha(x) &= \int_0^{+\infty} dx \sum_\alpha e_\alpha z_\alpha^{MF}(x) \\ &\quad - \beta \left( \sum_\alpha e_\alpha^2 \rho_\alpha^B \right) \left( \int_0^{+\infty} dx \Phi(x) \right) \times [1 + \mathcal{O}(\varepsilon_D \ln \varepsilon_D)] \end{aligned} \quad (4.9)$$

$\Phi(x)$  is given at leading order  $\varepsilon_D$  by (2.22), and the property

$$\int_0^{+\infty} dx \int d\mathbf{y} \kappa_D \tilde{\phi}^{(0)}(\kappa_D x, \kappa_D x', \kappa_D \mathbf{y}) = \frac{4\pi}{\kappa_D^2} \quad (4.10)$$

implies that

$$\int_0^{+\infty} dx \Phi(x) = \frac{4\pi}{\kappa_D^2} \int_0^{+\infty} dx' \sum_\gamma e_\gamma z_\gamma^{MF}(x') \quad (4.11)$$

Combination of (4.9) and (4.11) implies that (4.7) is indeed satisfied at leading order in  $\varepsilon_D$ .

### 4.3. Contact Theorem

Finally, we turn to the so-called contact theorem which gives the difference between the bulk thermodynamical pressure  $P^B$  and the kinetic pressure on the wall  $k_B T \sum_\alpha \rho_\alpha(x=b)$ . As shown for instance in ref. 3,

$$\begin{aligned} \beta P^B &= \sum_\alpha \rho_\alpha(x=b) - 2\pi \Delta_{\text{el}} \beta \left[ \int_b^{+\infty} dx \sum_\alpha e_\alpha \rho_\alpha(x) \right]^2 \\ &\quad - \beta \int_b^{+\infty} dx \sum_\alpha \rho_\alpha(x) \frac{\partial [e_\alpha^2 V_{\text{self}}]}{\partial x}(x) \\ &\quad - \beta \int_b^{+\infty} dx \int_b^{+\infty} dx' \int d\mathbf{y} \frac{\partial [v_w - v_B]}{\partial x}(x, x', \mathbf{y}) \\ &\quad \times \sum_{\alpha, \gamma} e_\alpha e_\gamma \rho_\alpha(x) \rho_\gamma(x') h_{\alpha\gamma}(x, x', \mathbf{y}) \end{aligned} \quad (4.12)$$

Since the global charge in the vicinity of a dielectric wall vanishes (see (4.7)), the second term in the r.h.s. of (4.12) is equal to zero.

The contact theorem implies that compensations between the various terms in the r.h.s. of (4.12) ensure that the bulk pressure is independent from  $b$  as well as from  $\epsilon_w$ ; in other words, the bulk pressure is independent from the specific forms of the interactions between particles and the wall, whether the latter interactions are purely geometric repulsions or coulombic couplings.

The above compensations can be checked at first order in the coupling parameter  $\epsilon_D$ , as shown in Appendix. On one hand, up to order  $\epsilon_D$ , the bulk pressure  $P^B$  is just the sum of the ideal-gas pressure plus the Debye correction<sup>(5)</sup>

$$\beta P^B = \sum_{\alpha} \rho_{\alpha}^B - \frac{\kappa_D^3}{24\pi} + \mathcal{O}(\rho \epsilon_D^2 \ln \epsilon_D) \quad (4.13)$$

where  $\rho$  is the order of magnitude of the  $\rho_{\alpha}^B$ 's. On the other hand, we calculate the r.h.s. of (4.12) by using the fact that the density profiles at first order in  $\epsilon_D$  obey the first BGY equation (2.1). In order to handle the contributions from the screened self-energy in  $\rho_{\alpha}(x)$  properly, the integrals are performed by using properties similar to (4.8) and derived from (3.15) and (3.16). Finally, after compensations of terms involving the dielectric response of the wall, the ideal-gas pressure arises and the remaining term is reduced to the difference between the kinetic pressure at the contact with a plain hard wall ( $\epsilon_w = 1$ ) and the ideal-gas pressure. The latter difference involves only the explicit value of the screened self-energy at the contact  $x = b$  with a plain hard wall. This value is independent from  $b$  and gives the term of order  $\epsilon_D$  in the bulk pressure (4.13).

## 5. CASE OF A PLAIN HARD WALL ( $\epsilon_w = 1$ )

### 5.1. Explicit Formulas

In this case the profile density is ruled only by the competition between Coulomb interactions in the fluid and the geometric deformation of screening clouds by the impenetrable wall. According to (3.17) and (3.20), the expression of the density profile is reduced to

$$\rho_{\alpha}^{HW}(x) = \rho_{\alpha}^B \left\{ 1 - \beta e_{\alpha}^2 \frac{\kappa_D}{2} L^{HW}(\kappa_D(x-b)) - \beta e_{\alpha} \Phi^{HW}(x) \right\} \quad (5.1)$$

In (5.1),  $L^{HW}$  can be explicitly calculated from (3.9) with the result (see ref. 8)

$$L^{HW}(u) = e^{-2u} \left[ \frac{1}{2u} + \frac{1}{u^2} + \frac{1}{2u^3} \right] - \frac{1}{u} K_2(2u) \quad (5.2)$$

where  $K_2$  is a Bessel function. According to (3.19),  $M^{HW}$  is reduced to  $\bar{M}^{HW}(x)$ . Thus  $M^{HW}$  is independent from the species  $\gamma$  and, according to (3.17),

$$\Phi^{HW}(x) = - \frac{2\pi\beta(\sum_{\gamma} \rho_{\gamma}^B e_{\gamma}^3)}{\kappa_D} \bar{M}^{HW}(\kappa_D(x-b)) \quad (5.3)$$

where  $\bar{M}^{HW}$  depends only on  $\kappa_D(x-b)$  since it is defined in terms of  $\bar{L}^{HW}(\kappa_D x; \kappa_D b)$  through (3.18) and  $\bar{L}^{HW}(\kappa_D x; \kappa_D b) = L^{HW}(\kappa_D(x-b))$  according to (3.11). Its expression at  $u = \kappa_D(x-b)$  coincides with (3.24) when  $\Delta_{el}$  is set to zero,

$$\bar{M}^{HW}(u) = \int_1^{+\infty} dt \left[ \frac{e^{-2tu} - 2te^{-u}}{1 - (2t)^2} \right] \frac{1}{(t + \sqrt{t^2 - 1})^2} \quad (5.4)$$

The large-distance behaviour of (5.4) reads

$$\bar{M}^{HW}(u) \underset{u \rightarrow \infty}{\sim} \frac{1}{2} \left[ \ln 3 - 2 + \frac{\pi}{\sqrt{3}} \right] e^{-u} \quad (5.5)$$

Since  $\bar{M}^{HW}$  is a positive function,  $\Phi^{HW}(x)$  has the same sign at all distances from the wall. This sign is determined by  $\sum_{\gamma} \rho_{\gamma}^B e_{\gamma}^3$ ,

$$\left( \sum_{\gamma} \rho_{\gamma}^B e_{\gamma}^3 \right) \Phi^{HW}(x) < 0 \quad (5.6)$$

## 5.2. Electric Layers

Near a hard wall the charge density profile takes the simple form

$$\sum_{\alpha} e_{\alpha} \rho_{\alpha}^{HW}(x) = -\beta \left( \sum_{\gamma} \rho_{\gamma}^B e_{\gamma}^3 \right) \frac{\kappa_D}{2} [L^{HW}(\kappa_D(x-b)) - \bar{M}^{HW}(\kappa_D(x-b))] \quad (5.7)$$

where  $-\bar{M}^{HW}$  is proportional to  $\Phi^{HW}$  according to (5.4). We have checked that (5.7) agrees with the result (32) in ref. 6. Since  $L^{HW}(0) = 1/3$  and  $\bar{M}^{HW}(0) = [\ln 3 + 1 - \pi/\sqrt{3}]/8$ ,  $L^{HW}(0) > \bar{M}^{HW}(0)$ , while  $L^{HW}$  and  $\bar{M}^{HW}$  are positive functions of  $x$  which decay respectively as  $\exp(-2\kappa_D x)/x$  and  $\exp(-\kappa_D x)$  when  $x$  goes to infinity. Therefore the expression (5.7) implies that the charge density profile is at least a double layer.

In a charge-symmetric plasma in a symmetric state, the local neutrality (4.5) and the vanishing of  $\Phi(x)$  (4.6), which are valid whatever the strength of the coupling inside the plasma may be and for any value of the densities, are retrieved at first order in  $\epsilon_D$  from our expressions. Indeed, according to (5.7) and (5.3),  $\sum_\alpha e_\alpha \rho_\alpha(x)$  and  $\Phi^{HW}(x)$  are both proportional to  $\sum_\gamma \rho_\gamma^B e_\gamma^3$  and this combination vanishes in any charge-symmetric plasma in a symmetric state. In a plasma with an even or odd number of species, for a particular set of densities which satisfies the constraint

$$\sum_\gamma \rho_\gamma^B e_\gamma^3 = 0 \tag{5.8}$$

the properties (4.5) and (4.6) happens to be valid at first order in  $\epsilon_D$ .

In a plasma which is not in a symmetric state, the charge density profile does not vanish and the sign of the charge density at the wall is fixed by the sign of  $\sum_\gamma \rho_\gamma^B e_\gamma^3$  (in the considered weak-coupling regime),

$$\left(\sum_\gamma \rho_\gamma^B e_\gamma^3\right) \sum_\alpha e_\alpha \rho_\alpha^{HW}(x=b) < 0 \tag{5.9}$$

The inequality (5.9) implies that if the magnitudes of positive charges is far larger than those of negative charges, then the layer at the contact with the wall is negatively charged. Moreover, the combination of (5.6) and (5.9) implies that

$$\Phi^{HW}(x=b) \sum_\alpha e_\alpha \rho_\alpha^{HW}(x=b) > 0 \tag{5.10}$$

### 5.3. Repulsion from the Wall for the Total Particle Density

According to the bulk local neutrality (2.3),

$$\sum_\alpha \rho_\alpha^{HW}(x) = \sum_\alpha \rho_\alpha^B - \frac{\kappa_D^3}{8\pi} L^{HW}(\kappa_D(x-b)) \tag{5.11}$$

Since  $L^{HW}$  is a positive function, the total particle density is lower than its bulk value at any point,

$$\sum_{\alpha} \rho_{\alpha}^{HW}(x) < \sum_{\alpha} \rho_{\alpha}^B \quad (5.12)$$

The total particle density undergoes a repulsion at any distance.

The repulsion from the wall also operates for every particle density when the electrostatic potential  $\Phi(x)$  vanishes, namely in the case of a charge-symmetric plasma in a symmetric state or in a plasma where the composition happens to satisfy (5.8). Indeed, according to (5.1), at any point

$$\rho_{\alpha}^{HW}(x) \left| \sum_{\gamma} \rho_{\gamma}^B e_{\gamma}^3 = 0 < \rho_{\alpha}^B \right. \quad (5.13)$$

The repulsion from the wall for every species when the potential drop with the bulk vanishes is interpreted as follows. According to (2.9), when  $\Phi(x=b) = 0$ , the ratio  $\rho_{\alpha}^{HW}(x=b)/\rho_{\alpha}^B$  is only determined by the screened self-energy which is the difference between the values of  $(e_{\alpha}^2/2)[\phi - v_B](\mathbf{r}, \mathbf{r})$  at the wall and in the bulk. According to (5.1), this difference is equal to  $(e_{\alpha}^2/2) \kappa_D L^{HW}(0)$ , which is positive. Thus, when there is no potential drop between the wall and the bulk, the immersion free-energy in the bulk is lower than its value at the hard wall: the charge surrounded by its screening cloud with global charge of opposite sign is more stable in the bulk than at the plain wall. In other words, for all species Coulomb screening is less efficient when polarization clouds are deformed by the presence of the hard wall. As an illustration, we consider a symmetric two-component plasma made of charges  $e$  and  $-e$ . According to charge-symmetry  $\rho_{+}(x) = \rho_{-}(x)$  and the profile density is drawn in Fig. 2a.

#### 5.4. Particle Density Profiles

The case of plasmas in a charge symmetric state has been discussed in the previous subsection. Here we consider the generic case where  $\sum_{\gamma} \rho_{\gamma}^B e_{\gamma}^3 \neq 0$ . Then, already at leading order in  $\epsilon_D$ ,  $\Phi^{HW}(x) \neq 0$  and  $\sum_{\alpha} e_{\alpha} \rho_{\alpha}(x) \neq 0$  so that the electrostatic potential created by the electric layer interplays with the geometric repulsion from the wall.

If  $\sum_{\gamma} \rho_{\gamma}^B e_{\gamma}^3 > 0$  then  $\Phi^{HW}(x) < 0$  for all  $x$  according to (5.6). Thus for all negatively charged species  $\alpha^{-}$  at any point, according to (5.1),

$$\rho_{\alpha^{-}}^{HW}(x) < \rho_{\alpha^{-}}^B \quad (5.14)$$

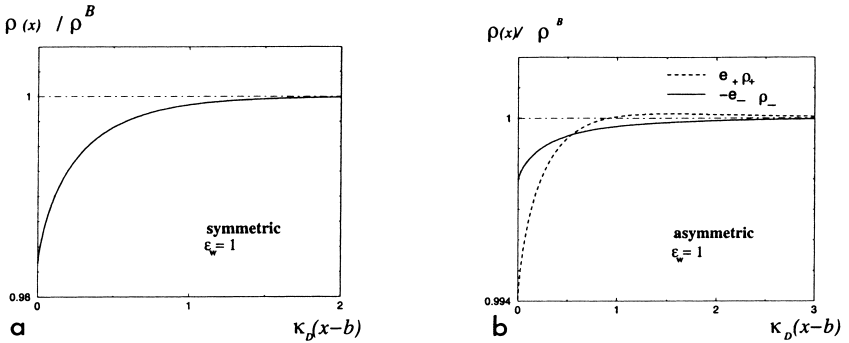


Fig. 2. Density profiles in a two-component plasma near a plain hard wall. If the plasma is symmetric (Fig. 2a)  $\Phi^{HW}(x) = 0$  and only the geometric repulsion from the wall is involved. The curve is the same as in ref. 9. If the plasma is charge asymmetric with  $e_+ = 2|e_-|$  (Fig. 2b),  $\Phi^{HW}(x = b) < 0 = \Phi^{HW}(x = +\infty)$  and the competition between the geometric repulsion from the wall and the attraction to the wall by  $\Phi^{HW}(x)$  for positive charges results into a double layer structure for  $\rho_+(x) - \rho_+^B$ . In Figs. 2a and b  $\kappa_D \beta e^2 = 0.01$  and  $\kappa_D b = 0.1$ .

because the geometric and electrostatic effects are both repulsive for them. For positively charged particles, since  $\bar{L}^{HW}(x)$  decays faster than  $\Phi^{HW}(x)$ , the attractive effect of the potential drop overcomes the wall repulsion at sufficiently large distances, and  $\rho_{\alpha^+}^{HW}(x) - \rho_{\alpha^+}^B$  becomes positive a priori at least at some distance  $x_0$  before decaying to zero when  $x$  goes to  $\infty$ ,

$$\rho_{\alpha^+}^{HW}(x) - \rho_{\alpha^+}^B \geq 0 \quad \text{for } x \geq x_0 \tag{5.15}$$

The result of the competition between the two effects is given by the density on the wall, which reads

$$\rho_{\alpha}^{HW}(x = b) = \rho_{\alpha}^B \left\{ 1 - \frac{1}{6} \beta \kappa_D \left[ e_{\alpha}^2 - e_{\alpha} \frac{3 \sum_{\gamma} \rho_{\gamma}^B e_{\gamma}^3}{4 \sum_{\gamma'} \rho_{\gamma'}^B e_{\gamma'}^2} \left( \ln 3 + 1 - \frac{\pi}{\sqrt{3}} \right) \right] \right\} \tag{5.16}$$

The sign of  $\rho_{\alpha}^{HW}(x = b) - \rho_{\alpha}^B$  depends on the particular composition of the plasma.

More precise results about the layer structure of  $\rho_{\alpha}^{HW}(x) - \rho_{\alpha}^B$  can be obtained in two special cases. First, in a two-component plasma made of charges  $e_+$  and  $e_-$ , the local neutrality in the bulk (2.3) enforces that

$$\rho_+^{HW}(x) = \rho_+^B \left\{ 1 - \frac{\beta \kappa_D e_+^2}{2} \left[ L^{HW}(\kappa_D(x-b)) - \left[ 1 + \frac{e_-}{e_+} \right] M^{HW}(\kappa_D(x-b)) \right] \right\} \tag{5.17}$$

The argument displayed after (5.7) shows that if  $e_+ > |e_-|$ ,  $\rho_+^{HW}(x) < \rho_+^B$  in a strip  $b < x < x_0$  whereas  $\rho_+^{HW}(x) > \rho_+^B$  for all  $x > x_0$ . As a conclusion, at leading order in  $\varepsilon_D$ , the wall repulsion still overcomes the electrostatic attraction arising from  $\Phi^{HW}$  for the positive charges near the wall and the profile density  $\rho_+^{HW}(x) - \rho_+^B$  has the structure of a double layer. This can be seen in Fig. 2b.

At last, we briefly discuss the case of a three-component plasma with  $\sum_\gamma e_\gamma^3 \rho_\gamma^B > 0$  and which is made for instance of species  $e_1 > 0$ ,  $e_2 > 0$  and  $e_3 < 0$ . Then  $\rho_3(x) < \rho_3^B$  according to (5.14). However, according to (5.16), the composition  $\{\rho_\gamma^B, e_\gamma\}_{\gamma=1,2,3}$  of the fluid may happen to be such that the electrostatic attraction of positive charges (proportional to  $e_\alpha$ ) overcomes the geometric repulsion from the wall at  $x = b$  (proportional to  $e_\alpha^2$ ) for the species which carries the positive charge  $e_i$  with the lowest magnitude, for instance  $e_2$ . Then  $\rho_2(x = b)$  may happen to be larger than  $\rho_2^B$  in spite of the wall geometric repulsion. If  $\rho_2(x = b) > \rho_2^B$ , according to (5.9) and the neutrality condition (2.3),  $\rho_1(x = b) < \rho_1^B$ , and  $\rho_1(x) - \rho_1^B$  contains at least a double layer.

## 6. GENERIC LOCAL PROPERTIES

### 6.1. Large-Distance Behaviours

As shown in Section 2 the density profile takes the form (1.8). The total screened self-energy  $e_\alpha^2 V_{\text{self}}^{\text{sc}}(x)$  is written in (3.6). Its decay at large distances  $e_\alpha^2 \exp(-2\kappa_D x)/4x$  (given by (3.10)) is independent from  $\Delta_{\text{el}}$  and is positive: far away from the wall, the screened self-energy is a repulsive effect, even if the electrostatic response of the wall upon one charge is attractive ( $\Delta_{\text{el}} > 0$ ). The contribution from the complete screened self-energy  $e_\alpha^2 V_{\text{self}}^{\text{sc}}$  to  $\rho_\alpha(x) - \rho_\alpha^B$  is drawn in Fig. 3.

The electrostatic potential decays only as  $\exp(-\kappa_D x)$  at large distances from the wall,

$$\Phi(x) \underset{x \rightarrow +\infty}{\sim} \Phi_{\text{as}} e^{-\kappa_D x} \quad (6.1)$$

The sign of  $\Phi_{\text{as}}$  depends on the composition  $\{e_\gamma, \rho_\gamma^B\}_{\gamma=1, \dots, n_s}$  as well as on  $\kappa_D b$  and  $\Delta_{\text{el}}$ . Indeed

$$\Phi_{\text{as}} = -\frac{2\pi\beta}{\kappa_D} \sum_\gamma e_\gamma^3 \rho_\gamma^B \{ \bar{M}_{\text{as}}(\kappa_D b, \Delta_{\text{el}}) + [M_\gamma - M](\tilde{x} = 0; \varepsilon_\gamma, \kappa_D b, \Delta_{\text{el}}) \} \quad (6.2)$$

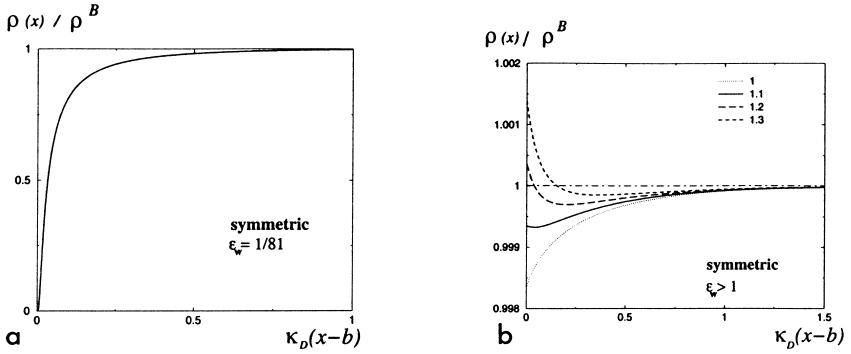


Fig. 3. Contribution from the complete screened self-energy  $e_\alpha^2 V_{\text{self}}^2$  to the profile density. In the case of a symmetric two-component plasma of charges  $e$  and  $-e$ ,  $\rho_+(x) = \rho_-(x) = \rho(x)$  and  $\Phi(x) = 0$  while  $\rho(x) = \rho^B \exp[-\beta e^2 V_{\text{self}}^{\text{sc}}(x)]$ . In Fig. 3a, where  $\epsilon_w < 1$ , both the electrostatic and geometric repulsions from the wall make  $\rho(x) < \rho^B$ . Figure 3b, where  $\epsilon_w > 1$ , displays the competition at short distances between the electrostatic attraction to the wall (which gets larger when  $\epsilon_w$  increases) and the geometric repulsion from the wall. In Fig. 3a,  $\kappa_D \beta e^2 = 0.1$  and  $\kappa_D b = 10^{-5}$  whereas in Fig. 3b,  $\kappa_D \beta e^2 = 0.01$ ,  $\kappa_D b = 0.1$  and the values of  $\epsilon_w$  are written in the figure.

where, in the limit  $\eta \equiv \kappa_D b = 0$ ,  $\bar{M}_{\text{as}}$  is obtained from (3.24)

$$\bar{M}_{\text{as}}(\eta = 0, \Delta_{\text{el}}) = \frac{1}{8} \frac{1 - \Delta_{\text{el}}^2}{1 + \Delta_{\text{el}} + \Delta_{\text{el}}^2} \left\{ \frac{\pi}{\sqrt{3}} + (1 + 2\Delta_{\text{el}}) \ln 3 + 2 \frac{(1 - \Delta_{\text{el}}^2)}{\Delta_{\text{el}}} \ln(1 - \Delta_{\text{el}}) \right\} \tag{6.3}$$

while  $[M_\gamma - M](\tilde{x} = 0; \epsilon_\gamma, \eta = 0, \Delta_{\text{el}})$  is calculated from (3.23).

In an asymmetric plasma or a charge-symmetric plasma with at least four components and in an asymmetric state, as far as the density profile of one species is concerned, the  $\exp(-2\kappa_D x)/x$  tail of the screened self-energy is always overcome by the effect of  $-e_\alpha \Phi(x)$ ,

$$\rho_\alpha^{\text{asym}}(x) \underset{x \rightarrow +\infty}{\sim} \rho_\alpha^B [1 - \beta e_\alpha \Phi_{\text{as}} e^{-\kappa_D x}] \tag{6.4}$$

On the contrary, in a symmetric two-component plasma or in a charge-symmetric plasma with more than two components and in a symmetric state (see definition (4.4)),  $\Phi(x) = 0$  and

$$\rho_\alpha^{\text{sym}}(x) \underset{x \rightarrow +\infty}{\sim} \rho_\alpha^B \left[ 1 - \beta e_\alpha^2 \frac{e^{-2\kappa_D x}}{4x} \right] \tag{6.5}$$

However, because of the bulk local neutrality, the influence of  $\Phi(x)$  at large distances disappears in the total particle density  $\sum_{\alpha} \rho_{\alpha}(x)$  even in the case of an asymmetric plasma

$$\sum_{\alpha} \rho_{\alpha}(x) \underset{x \rightarrow +\infty}{\sim} \sum_{\alpha} \rho_{\alpha}^B - \frac{\kappa_D^2}{16\pi} \frac{e^{-2\kappa_D x}}{x} + \mathcal{O}\left(\frac{e^{-3\kappa_D x}}{x}\right) \quad (6.6)$$

The total particle density is submitted to an effective repulsion far away from the wall. On the contrary, the charge density at large distances is determined by  $\Phi(x)$ ,

$$\sum_{\alpha} e_{\alpha} \rho_{\alpha}(x) \underset{x \rightarrow +\infty}{\sim} -\frac{\kappa_D^2}{4\pi} \Phi_{as} e^{-\kappa_D x} \quad (6.7)$$

When approaching the bulk region, the charge density vanishes with a sign ruled by the composition of the Coulomb fluid.

## 6.2. Effect of the Wall Dielectric Response

The three effects which interplay in the density profiles when  $\epsilon_w \neq 1$  have been discussed in Sections 5.3 and 6.1. Here we consider an asymmetric two-component plasma with  $e_+ = -2e_-$  and we comment briefly the corresponding figures for the profiles of particle and charge densities.

First we turn to the density profiles. When  $\epsilon_w = 1$  the density at the wall ( $x = b$ ) differs from its bulk value only by a term of order  $\epsilon_D = \kappa_D \beta e^2 / 2$  (see Fig. 2b). When  $\epsilon_w < 1$  the electrostatic repulsion from the wall makes all density profiles at the wall ( $x = b$ ) vanish exponentially fast when  $b$  goes to zero (see Fig. 4a). When  $\epsilon_w > 1$  the density at  $x = b$  increases as  $\epsilon_w$  gets larger because of the electrostatic attraction to the wall (see Fig. 4b). Subsequently, the difference  $\rho_+(x) - \rho_+^B$ , which has a double-layer structure when  $\epsilon_w \leq 1$ , exhibits a threefold-layer structure when  $\epsilon_w$  becomes sufficiently large.

The charge density profile  $C(x) = e_+ \rho_+(x) + e_- \rho_-(x)$  obeys the same evolution when  $\epsilon_w$  varies. If  $\epsilon_w = 1$ , according to (5.6), the condition  $\rho_+ e_+^3 + \rho_- e_-^3 > 0$  implies that  $\Phi^{HW}(x = b) < 0$  and enforces the double layer  $\ominus \oplus$  shown in Fig. 5 and discussed after (5.7). This double layer arises from the balance between the electrostatic force associated with  $\Phi(x)$  and created by  $C(x)$  itself and the geometric repulsion from the wall due to the deformation of screening clouds. When  $\epsilon_w < 1$ , the extra electrostatic repulsion from the wall does not destroy the double layer and only enforces

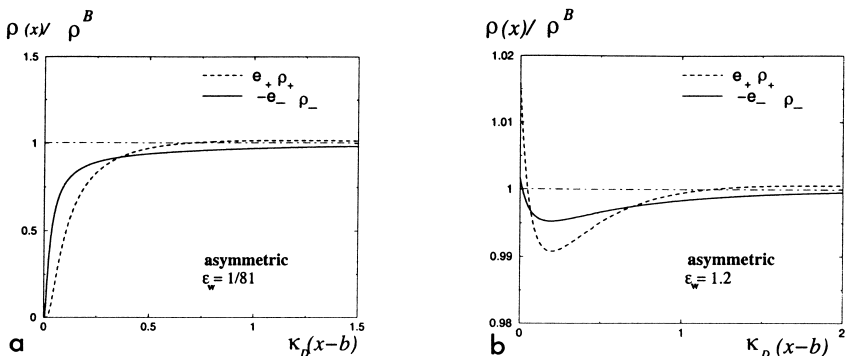


Fig. 4. Density profiles in an asymmetric two-component plasma ( $e_+ = 2|e_-|$ ) when  $\epsilon_w$  varies. In Fig. 4a,  $\kappa_D \beta e^2 = 0.1$  and  $\kappa_D b = 10^{-5}$ , whereas in Fig. 4b,  $\kappa_D \beta e^2 = 0.01$ ,  $\kappa_D b = 0.1$  and the values of  $\epsilon_w$  are given in the figure.

the vanishing of  $C(x)$  at  $x = 0$  when  $b = 0$  (see Fig. 6a). When  $\epsilon_w > 1$ , in the case of positive charges, the electrostatic self-attraction to the wall competes with the opposite effect of  $\Phi(x)$  and for high enough values of  $\epsilon_w$ ,  $C(x)$  contains three layers  $\oplus \ominus \oplus$  (see Fig. 6b). When  $\epsilon_w$  becomes far larger, the electrostatic self-attraction to the wall is so strong that the sign of  $\Phi(x)$  at large distances changes and again there appears a double layer  $\oplus \ominus$  but with signs reversed with respect to the situation when  $\epsilon_w = 1$  (see Fig. 6c).

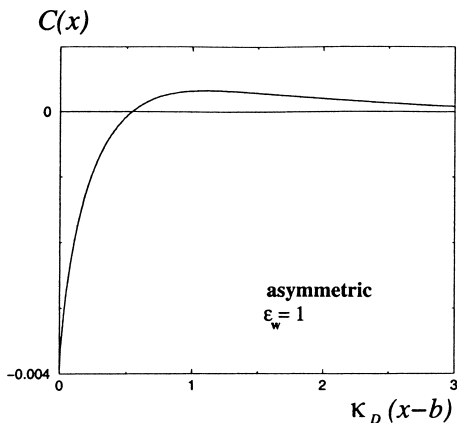


Fig. 5. Double layer of the charge density profile  $C(x) = e_+ \rho_+(x) + e_- \rho_-(x)$  for the asymmetric two-component plasma already considered in Fig. 2.  $\sum_\gamma \rho_\gamma^B e_\gamma^3 > 0$  in this case and inequality (5.9) can be checked.

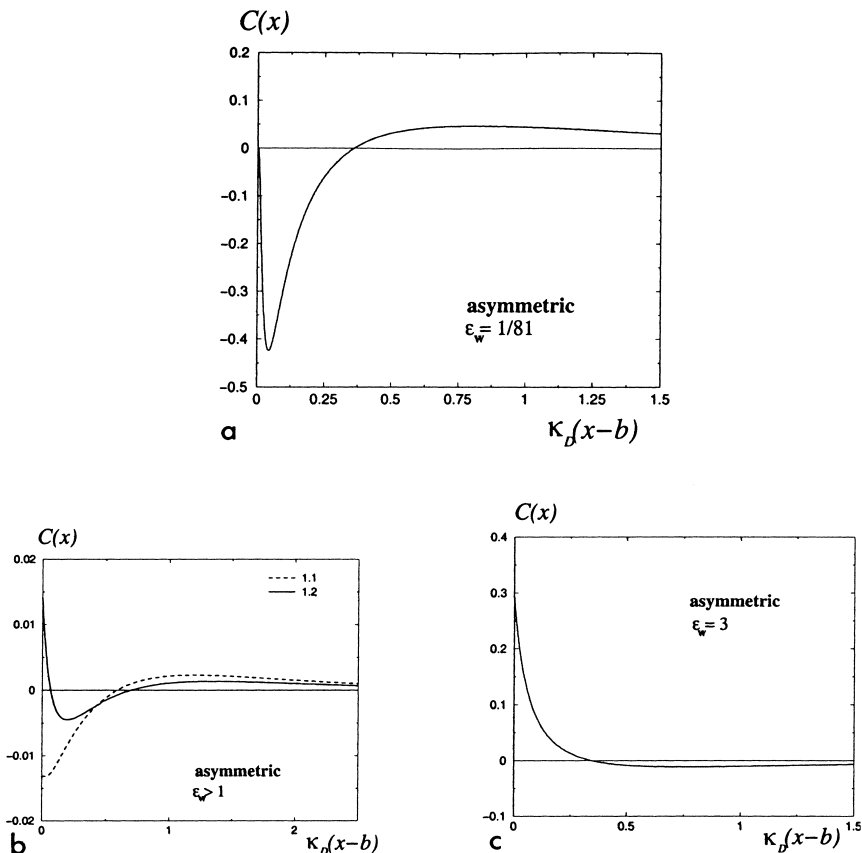


Fig. 6. Charge density profiles in the same two-component plasma as in Fig. 5. In Fig. 6a,  $\kappa_D \beta e^2 = 0.1$  and  $\kappa_D b = 10^{-5}$  and in Figs. 6b and c,  $\kappa_D \beta e^2 = \kappa_D b = 0.1$ .

## APPENDIX

In the present appendix we show that the contact theorem (4.12) is satisfied by the profile densities found at first order in  $\epsilon_D$ . First, we consider a plain hard wall ( $\Delta_{\text{el}} = 0$ ) and then we turn to the case of a wall with a dielectric response.

In the case of a plain hard wall, the r.h.s. side of (4.12) is reduced to the kinetic pressure on the wall

$$\beta P^B = \sum_{\alpha} \rho_{\alpha} |_{\Delta_{\text{el}}=0}(x=b) \quad (\text{A.1})$$

According to the bulk local neutrality (2.3) the contribution from  $\Phi(b)$  to  $\sum_{\alpha} \rho_{\alpha}|_{A_{el}=0}(x=b)$  is zero, and, according to (5.11),

$$\sum_{\alpha} \rho_{\alpha}|_{A_{el}=0}(x=b) = \sum_{\alpha} \rho_{\alpha}^B - \beta \sum_{\alpha} \rho_{\alpha}^B e_{\alpha}^2 V_{\text{self}}^{sc}|_{A_{el}=0}(x=b) + \mathcal{O}(\rho \varepsilon_D^2 \ln \varepsilon_D) \quad (\text{A.2})$$

Since  $V_{\text{self}}^{sc}|_{A_{el}=0}(x=b) = -\kappa_D/6$  (see Section 5), the kinetic pressure (A.2) on the wall does coincide with the value (4.13) of the bulk pressure at first order in  $\varepsilon_D$ .

Now we turn to the case of a wall with a dielectric response. First, the last integral in the r.h.s. side of (4.12) can be written as the sum  $I_W - I_B$  where

$$I_W = \int_b^{+\infty} dx \sum_{\alpha} \rho_{\alpha}(x) J_{W,\alpha}(x) \quad (\text{A.3})$$

and  $J_{W,\alpha}(x)$  is the integral in the r.h.s. of the first BGY equation (2.1).  $I_B$  and  $J_{B,\alpha}(x)$  are defined in a similar way. The value  $J_{W,\alpha}^{MF}(x)$  of  $J_{W,\alpha}(x)$  in the mean-field approximation is given in (2.7). By use of the definitions (1.4) and (2.10), it can be rewritten as

$$J_{W,\alpha}^{MF}(x) = -\beta e_{\alpha}^2 \frac{\partial}{\partial x} [V_{\text{self}}^{sc}(x) - V_{\text{self}}(x)] \quad (\text{A.4})$$

Therefore

$$\begin{aligned} I_W^{MF} - \beta \int_b^{+\infty} dx \sum_{\alpha} \rho_{\alpha}(x) \frac{\partial [e_{\alpha}^2 V_{\text{self}}]}{\partial x}(x) \\ = -\beta \int_b^{+\infty} dx \sum_{\alpha} \rho_{\alpha}(x) \frac{\partial [e_{\alpha}^2 V_{\text{self}}^{sc}]}{\partial x}(x) \end{aligned} \quad (\text{A.5})$$

The r.h.s. of equality (A.5) does not involve the bare self-energy  $V_{\text{self}}(x)$  and it is calculated by inserting the expression (1.8) of  $\rho_{\alpha}(x)$  in terms of the screened self-energy and the electrostatic potential  $\Phi(x)$ . After an integration by parts, we notice that, according to (3.15) and (3.16),

$$\int_b^{+\infty} dx \exp[-\beta e_{\alpha}^2 V_{\text{self}}^{sc}(x)] \frac{\partial \Phi(x)}{\partial x} = \left[ \int_b^{+\infty} dx \frac{\partial \Phi(x)}{\partial x} \right] \times [1 + \mathcal{O}(\varepsilon_D \ln \varepsilon_D)] \quad (\text{A.6})$$

Then the local neutrality in the bulk (2.3) implies that the sum (A.5) is equal to

$$\sum_{\alpha} \rho_{\alpha}^{\text{B}} - \sum_{\alpha} \rho_{\alpha}(x=b) + \mathcal{O}(\rho \varepsilon_D^2 \ln \varepsilon_D) \quad (\text{A.7})$$

Second, we calculate  $I_{\text{B}}$  which is defined in terms of

$$J_{\text{B},\alpha} \equiv -\beta e_{\alpha} \int_b^{+\infty} dx' \int dy \frac{\partial v_{\text{B}}}{\partial x}(x-x', \mathbf{y}) \sum_{\gamma} e_{\gamma} \rho_{\gamma}(x') h_{\alpha\gamma}(x, x', \mathbf{y}) \quad (\text{A.8})$$

as in (A.3). In fact, the difference

$$h_{\alpha\gamma}(x, x', \mathbf{y}) - h_{\alpha\gamma}|_{\Delta_{\text{el}}=0}(x, x', \mathbf{y}) \quad (\text{A.9})$$

gives a vanishing contribution to  $I_{\text{B}}$ . Indeed, the mean-field value (2.5) of  $h_{\alpha\gamma}$  is proportional to  $\phi^{(0)}$  and, according to (3.2) and (3.4),  $\phi^{(0)} - \phi^{(0)}|_{\Delta_{\text{el}}=0}$  is bounded by a product of functions  $f(x, x')g(\mathbf{y})$  where  $g(\mathbf{y})$  is integrable while  $f(x, x')$  decays exponentially fast in all directions in the plane of variables  $(x, x')$ . As a consequence

$$\frac{\partial v_{\text{B}}}{\partial x}(x-x', \mathbf{y}) \sum_{\alpha, \gamma} e_{\alpha}^2 e_{\gamma}^2 \rho_{\alpha}(x) \rho_{\gamma}(x') [\phi^{(0)}(x, x', \mathbf{y}) - \phi^{(0)}|_{\Delta_{\text{el}}=0}(x, x', \mathbf{y})] \quad (\text{A.10})$$

is absolutely integrable in the space  $(x, x', \mathbf{y})$ . Moreover,  $\phi^{(0)} - \phi^{(0)}|_{\Delta_{\text{el}}=0}$  is symmetric under exchange of  $x$  and  $x'$  whereas  $\partial v_{\text{B}}/\partial x$  is antisymmetric under the same exchange. Subsequently, the contribution from the difference (A.9) to  $I_{\text{B}}$  is just zero. Moreover, when  $\Delta_{\text{el}}=0$  the self-energy is bounded for all  $x$ 's ranging from 0 to  $+\infty$  so that, according to (3.17),

$$\rho_{\alpha}(x) - \rho_{\alpha}|_{\Delta_{\text{el}}=0}(x) = \rho_{\alpha}^{\text{B}} \{ \exp[-\beta e_{\alpha} V_{\text{self}}^{\text{sc}}(x)] - 1 + \mathcal{O}_{\text{exp}}(\varepsilon_D) \} \quad (\text{A.11})$$

and, according to (3.15) and (3.16),  $\rho_{\alpha}(x) - \rho_{\alpha}|_{\Delta_{\text{el}}=0}(x)$  contributes to  $I_{\text{B}}$  by a term of order  $\rho \varepsilon_D^2 \ln \varepsilon_D$ , as well as  $\rho_{\gamma}(x') - \rho_{\gamma}|_{\Delta_{\text{el}}=0}(x')$ . Eventually,

$$I_{\text{B}} = I_{\text{B}}|_{\Delta_{\text{el}}=0} + \mathcal{O}(\rho \varepsilon_D^2 \ln \varepsilon_D) \quad (\text{A.12})$$

Since the Ursell function  $h_{\alpha\gamma}|_{\Delta_{\text{el}}=0}$  obeys the BGY hierarchy with  $v_{\text{w}}$  replaced by  $v_{\text{B}}$ , a calculation similar to that performed for  $I_{\text{W}}$  leads to

$$I_{\text{B}}|_{\Delta_{\text{el}}=0} = \sum_{\alpha} \rho_{\alpha}^{\text{B}} - \sum_{\alpha} \rho_{\alpha}|_{\Delta_{\text{el}}=0}(x=b) + \mathcal{O}(\rho \varepsilon_D^2 \ln \varepsilon_D) \quad (\text{A.13})$$

According to (A.2), the r.h.s. of (A.13) coincides with the opposite of the term of order  $\varepsilon_D$  in the bulk pressure. Therefore (A.13) leads to

$$I_B = \frac{\kappa_D^3}{24\pi} + \mathcal{O}(\rho\varepsilon_D^2 \ln \varepsilon_D) \quad (\text{A.14})$$

Eventually, the sum of the terms in the r.h.s. of (4.12) does coincide with the value (4.13) of  $\beta P^B$ .

## REFERENCES

1. A. Alastuey, The one component plasma near a hard wall: Weak coupling limit with image forces, *Mol. Phys.* **50**:33 (1983).
2. A. Alastuey and A. Perez, Virial expansions for quantum plasmas: Fermi-bose statistics, *Phys. Rev. E* **53**:5714 (1996).
3. S. Carnie and D. Chan, The statistical mechanics of the electrical double layer: Stress tensor and contact conditions, *J. Chem. Phys.* **74**:1293 (1981).
4. F. Cornu, Quantum plasmas with or without a uniform field. II Exact low-density free energy, *Phys. Rev. E* **58**:5293 (1998).
5. P. Debye and E. Hückel, Zur Theory der Elektrolyte, *Physik. Z.* **9**:185 (1923).
6. R. L. Guernsey, Correlation effects in semi-finite plasmas, *Phys. Fluids* **13**:2089 (1970).
7. J. D. Jackson, *Classical Electrodynamics* (Wiley, New York, 1962).
8. B. Jancovici, Classical Coulomb systems near a plane wall. I. *J. Stat. Phys.* **28**:43 (1982).
9. B. Jancovici, Classical Coulomb systems near a plane wall. II. *J. Stat. Phys.* **29**:263 (1982).
10. Ph. Martin, Sum rules in charges fluids, *Rev. Modern Phys.* **60**:1075 (1988).
11. L. Onsager and N. T. Samaras, The surface tension of Debye-Hückel electrolytes, *J. Chem. Phys.* **2**:528-536 (1934).